Transcriptomic insights into innate immunity responding to red rot disease in red alga Pyropia yezoensis

Lei Tang
Ocean University of China https://orcid.org/0000-0002-3652-205X
Liping Qiu
Ocean University of China
Cong Liu
Ocean University of China
Zhaolan Mo
Chinese Academy of Fishery Science Yellow Sea Fisheries Research Institute
Yunxiang Mao (yxmao@ouc.edu.cn)

Research article

Keywords: Transcriptome; Pyropia yezoensis; innate immune systems; infection; Pythium porphyrae

Posted Date: August 30th, 2019

DOI: https://doi.org/10.21203/rs.2.13745/v1

Version of Record: A version of this preprint was published at International Journal of Molecular Sciences on November 27th, 2019. See the published version at https://doi.org/10.3390/ijms20235970.

Abstract

Pyropia yezoensis , one of the most economically important marine algae, suffers from the biotic stress of oomycete necrotrophic pathogen Pythium porphyrae . However, little is known about the molecular defensive mechanisms employed by Pyr. yezoensis during the infection process. In the present study, we defined three stages of infection based on the histopathological features and photosynthetic physiology. Transcriptomic analysis was carried out at different stages of infection to identify the genes related to the innate immune system in Pyr. yezoensis . In total, 2139 up-regulated genes and 1672 down-regulated genes were identified from all the infected groups. Three up-regulated genes encoding extracellular lectin domains (one C-type lectin gene and two L-type lectin genes) were predicted to be p attern r ecognition r eceptors (PRRs) that activate PAMP-triggered immunity (PTI). Several defense mechanisms that were typically regarded as PTI in plants were induced during the infection. These include defensive and protective enzymes, heat shock proteins, secondary metabolites, cellulase, and protease inhibitors. Twenty-three genes that encode typical plant R protein domains (LRR, NBS, or TIR) were found to be up-regulated after infection. They were likely to be regarded as candidates of putative R proteins in Pyr. yezoensis . As a part of E ffector- t riggered i mmunity (ETI), expression of genes related to the ubiquitin-proteasome system (UPS) and hypersensitive cell death response (HR) increased significantly during the infection. The current study suggests that, similar to plants, Pyr. yezoensis possesses a relatively complete innate immune system to counter the invasion of necrotrophic pathogen Pyt. porphyrae . However, innate immunity genes of Pyr. yezoensis appear to be more ancient in origin compared to that in plants.

Background

Plant suffer from a variety of diseases that are caused by fungi [1-3], oomycetes[4, 5], bacteria[6] and viruses [7-9]. It is evident that plants rely on their innate immune system to resist infection by the pathogens. Jones proposed a four-phased ‘zigzag’ model to illustrate how the plants’ innate immune system fights against the pathogen[10]. At the onset, the plant recognizes the pathogen-associated molecular patterns (PAMPs) by their transmembrane pattern recognition receptors (PRRs) to activate PAMP-triggered immunity (PTI). PTI includes callose deposition[11, 12], cell-wall thickening[13, 14] and reactive oxygen species (ROS) production[15, 16], to control the colonization of pathogen nonspecifically. Next, pathogen interferes with the PTI by its effectors, resulting in effector-triggered susceptibility (ETS) of the plant. Further, the plant specifically recognizes effectors via R proteins either directly or indirectly to activate ETI[17]. ETI can amplify PTI and enhance the resistance by activating the hypersensitive cell death in the plant. Finally, pathogen represses ETI by modifying or acquiring new effectors that prevent the recognition of R proteins, further inducing ETS.

Similar to plants, algae can potentially get infected by a variety of pathogens[18-20]. Several defense mechanisms have been identified in Phaeophyta such as *Ectocarpus siliculosus* and *Saccharina japonica*. *E. siliculosus- Eurychasma dicksonii* was used as a model of Phaeophyta-oomycete interaction [21, 22]. *E. siliculosus* responds to infection by strengthening the cell wall, producing protease inhibitors,

ROS and by halogen metabolism[23, 24]. *Laminaria digitate*, a model organism in macroalgae immune study, activates ROS[25, 26], releases free fatty acid [27], and employs halogen metabolism and defense gene expression[28] in response to bacterial infection. Another important brown alga *S. japonica* could get infected by several alginic acid-decomposing bacterial strains[29]. *S. japonica* generates ROS after successful recognition of bacterial PAMPs flg22, to fight the pathogen [30]. Furthermore, hypersensitive programmed cell death (PCD) was observed in *S. japonica* post-infection [30].

Pyropia yezoensis, one of the economically important red algae massively cultivated in East Asia, is susceptible to *Alternaria* [31], *Olpidiopsis porphyrae* [32], and *Phoma sp.* [33]. Red rot disease, caused by necrotrophic oomycete pathogen *Pythium porphyrae* [34], is lethal to the gametophyte of *Pyr. yezoensis*. The symptoms first appear as red needle-sized lesions on the surface of the thallus, followed by expansion to the whole thallus in 2–3 days, thus leading to large scale necrosis of *Pyr. yezoensis* [35]. Interestingly, few surviving cells surrounded by *Pyt. porphyrae* hyphae could be observed in the lesion [36] which indicates that *Pyr. yezoensis* does possess a defense mechanism to resist the infection. However, little is known about the immune system in *Pyr. yezonesis*. It is reported that *Pyropia tenera* could produce reactive oxygen species (ROS), inducing HSPs and cell wall-associated hydrolases to prevent the spread of oomycete pathogen [37]. In *Pyr. yezoensis*, proteins related to photosynthesis, energy, and carbohydrate metabolism are shown to be suppressed in response to *Pyt. porphyrae* infection [38].

High throughput sequencing techniques, such as RNA-seq, is a powerful tool to analyze global gene expression during plant-pathogen interaction. In the current study, differentially expressed genes in the distinct stages of *Pyr. yezoensis* infection was investigated by transcriptomic analysis. *Pyr. yezoensis* complete innate immune system that includes PRRs, PTI mechanism, putative R proteins, and ETI mechanisms are described.

Methods

Algae and pathogen

A lab-cultured pure line RZ of *Pyr. yezoensis* was used as the host in the infection test. Gametophytes were cultured under 40 μmol photons m^{-2} s^{-1} at 10°C and a photoperiod of light: dark=12h:12h to obtain thalli. Boiled seawater supplemented with Provasoli's enrichment solution medium (PES) [70] was used as a growth medium.

The *Pyt. porphyrae* strain of NBRC33253 was used as a pathogen in the infection test. The hyphae of NBRC33253 were cultured at 24°C in a medium of 50% seawater glucose-glutamate medium (SGG)[71]. Zoospores of NBRC33253 were induced as described previously[72].

Infection test and sampling

Healthy RZ thalli (0.4 g fresh weight) (1.2±0.2 cm in width, 9.3±1.1 cm in length) were exposed to 200 mL zoospore suspension (1×10^5 zoospores mL^{-1}) in a flask with PES incubated under 40 μmol photons m^{-2}

s^{-1} at 15°C and a photoperiod of light: dark=12h:12h for 10 days. After lesions appeared, the infected thallus could be divided into two areas: the lesion and the area beyond the lesion. The two areas were separated using a sterile blade under a stereomicroscope and collected as groups of severely and slightly infected stages. Healthy *Pyr. yezoensis* thalli were collected as a control group. All samples were collected and stored in liquid nitrogen. Three biological replicates were performed in each group.

Maximum PSII quantum yield

The thalli of the three groups collected and stored as described in the previous step were used to measure the maximum PSII quantum yield by FluorCam 800MF (Photon Systems Instruments, Czech Republic). Minimal fluorescence (F_0) was obtained after dark adaption for 15 minutes. Maximal fluorescence in the dark-adapted state (F_M) was measured after illuminating with a saturating pulse (2000μmol photons m^{-2} s^{-1}). Maximum PSII quantum yield was calculated using the formula $F_V/F_M = (F_M - F_0)/F_M$. F_V/F_M of a different area in the infected thallus was analyzed by FluorCam software7 version 1.2.5.7 on manual mode. Three biological replicates were performed in each group.

RNA extraction, construction of cDNA library, and sequencing

Nine samples (collected from three groups with three replicates) were ground in liquid nitrogen and total RNA was extracted using the Plant RNA Kit (Omega) following the manufacturer's instructions. DNase I(Omega) was used to digest the DNA RNA extraction. The quantity and integrity/quality of the total RNA extracted was examined on a Nanodrop and Agilent 2100 bioanalyzer (Agilent Technologies, Inc., Santa Clara, CA).

1μg of total RNA was used to construct a cDNA library using VAHTS^{TM} mRNA-seq V3 Library Prep Kit for Illumina (Vazyme biotech co., ltd.) following the manufacturer's protocol. High-throughput sequencing was performed on the Illumina HiSeq 2000 platform in a paired-end 150 bp run.

RNA-seq analysis

The genome of *Pyropia yezoensis* was used as a reference genome to filter the reads from infected groups. Genome index was built using Bowtie2 and clean reads were aligned with the genome of *Pyr. yezoensis* using Tophat software. Genes expression was quantified by cuffquant and the normalized by cuffnorm to obtain the value of the number of fragments per kilobase per million (FPKM) for each group. Cuffdiff was used to identify differentially expressed genes and the data was manually screened to identify the significant differentially expressed genes with thresholds of FPKM > 3 and >1.5-fold (or < 0.67 fold) change.

GO and KEGG enrichment analysis

GO enrichment analysis was performed using OmicShare tools, which is a free online platform for data analysis (www.omicshare.com/tools). KEGG pathway analysis was performed using OmicShare tools

(www.omicshare.com/tools).

Prediction of secretory proteins

Differentially expressed secretory proteins in *Pyr. yezoensis* were predicted by the following steps[73].

1) All differentially expressed protein sequences were submitted to SignalP 4.1 online (http://www.cbs.dtu.dk/services/SignalP/) to identify proteins containing a signal peptide[74, 75]. Default parameters were used in this experiment.

2) TMHMM v2.0 (http://www.cbs.dtu.dk/services/TMHMM/) was used to analyze whether transmembrane domains were present in the proteins obtained from SignalP 4.1. Thus, transmembrane proteins were separated from secretory proteins.

3Subcellular localization was analyzed by Target P 1.1 Server (http://www.cbs.dtu.dk/services/TargetP/). Proteins localized in mitochondria, chloroplasts, and other subcellular locations were identified and distinguished. Extracellular secretory proteins were obtained for further analysis.

Prediction of LRR, NBS, TIR domain containing genes

HMMsearch was used to predict proteins that had LRR, NBS, and TIR domains in *Pyr. yezoensis*. Seeding sequence alignments of NBS(PF00931), LRR(PF00560), and TIR(PF01582) were generated on the PFAM website (http://pfam.xfam.org) in Stockholm format. HMMbuild, from HMMER package 3.1b2, was used to create Hidden Markov model (HMM) of the three domains. The profile of HMM was used to search for transcripts with a cut-off E-value of 10^{-5}.

Multicolor fluorescence imaging

MCFI of healthy and infected thallus was performed using Multi-color FluorCam (Photon Systems Instruments, Czech Republic). The thallus was tiled with a little boiled seawater in Petri dishes and then kept on the sample table. The excitation wavelength used was 355 nm. The fluorescence spectra of blue (F440), green (F520), red (F690), and far red (F740) were collected. Fluorescence image was displayed with a false-color scale by the FluorCam software7 version 1.2.5.7. Further, F520 of a different area in the infected thallus was analyzed by FluorCam software7 version 1.2.5.7 on manual mode. Three biological replicates were performed in each group.

Phylogenetic analysis

Protein sequences of genes related to lectin, R proteins, cellulase, RBOH and metalloproteinase inhibitors were collected from GenBank. The GenBank accession number of all sequences are listed in Table S1. Protein sequences from the current study were used as queries to blast in GenBank using the default parameters. All hits were filtered employing two criteria: a) the protein was annotated clearly in NR or

KEGG database; b) the protein was from any model plant species and phylogenetically related species. Protein sequences were aligned using CLUSTAL W software and neighbor-joining trees were constructed in MEGA 7.0.

Results

A global view of the transcriptome

The definition of infection process was described in [Additional files 1]. In total, 2139 up-regulated genes and 1672 down-regulated genes were identified within the control group, slightly infected stage and severely infected stages. As shown in Fig 1, 1312 up-regulated genes were found to be unique slightly infected thallus in comparison with the healthy sample. Further, 698 up-regulated genes were unique in severely infected stage compared to the slightly infected stage of the thallus. KEGG enrichment analysis showed that the function in the two comparisons was different. Unique up-regulated genes in comparison with the healthy and slightly infected stage were mainly related to amino acid metabolism and glycan degradation, but unique up-regulated genes when the slightly and severely infected stages were compared, were mainly related to the biosynthesis of secondary metabolites. Among the down-regulated genes, 884 genes were unique in the comparison of healthy and slightly infected stage and 749 genes were unique in the comparison of slightly and severely infected stage. KEGG enrichment revealed that the function of unique down-regulated genes between the two comparisons was related to several fundamental physiological processes. Unique down-regulated genes observed when comparing the healthy and slightly infected stages were mainly related to cell cycle, amino acid degradation, and signaling pathways. Unique down-regulated genes noted when comparing slightly and severely infected stages were mainly related to photosynthesis and protein synthesis.

Lectins in *Pyr. yezoensis*

Successful recognition of PAMPs-PRRs is the initial step in innate immune response[10]. Genes containing typical PRR functional domains (LRR, Lectin, EGF, and lysine motif) were searched using the PFAM annotation. In *Pyr. yezoensis*, lectin-containing genes, and LRR-containing genes were seen whereas EGF- or lysine motif-containing genes were unable to find. Further analysis revealed that only lectin-containing genes encode for the transmembrane proteins with extracellular functional lectin domain. Transcriptome analysis also showed that the expression of three lectin-containing genes was significantly increased during infection. These up-regulated genes were expressed specifically in different infected stage: C-type lectin-containing gene py02002.t1 was up-regulated only in the slightly infected stage by 1.72-fold; two L-type lectin-containing genes py02275.t1 and py02843.t1 were up-regulated only in the severely infected stage by 2.36- and 2.44-folds, respectively.

PTI mechanism in *Pyr. yezoensis*

ROS-related genes

Expression pattern of the respiratory burst and cellular anti-oxidation related genes that include NADPH-oxidase and antioxidant enzymes is represented in Fig 2. In *Pyr. yezoensis*, NADPH-oxidase gene py00308.t1 up-regulated constantly during the process of infection. The expression of py00308.t1 increased by 1.68- and 2.36-folds in slightly and severely infected stages, respectively, compared to that in the healthy group. The up-regulation of antioxidases, such as peroxidase (POD), catalase (CAT), and superoxide dismutase (SOD), were related to scavenging extra ROS. Expression of POD in *Pyr. yezoensis* increased by 1.6-fold and 2.63-fold during the infection. Two CAT genes were found to be upregulated. CAT-1 strictly up-regulated in the severely infected stage (FC=1.87) and CAT-2 up-regulated in both the slightly (FC=1.70) and severely infected stages (FC=1.76). One gene of SOD up-regulated in both slightly (FC=1.60) and severely infected stages (FC=1.65).

Cellulase

From the transcriptome data of *Pyr. yezoensis*, we identified a cellulase enzyme that could degrade the cellulose which is the major component of *Pyt. porphyrae* cell wall. Compared with the healthy *Pyr. yezoensis*, the expression of py05706.t1 increased by 3.84-fold and 3.57-fold in slightly and severely infected stages (Fig. 2). Bioinformatic analysis showed that py05076.t1 had a signal peptide at the N-terminus and is predicted to be a secretory protein by Target P. It is likely that *Pyr. yezoensis* secretes py05076.t1 as an extracellular cellulase.

Metalloproteinase inhibitor

The expression of transcript py03343.t1, annotated as a metalloproteinase inhibitor increased by 2.13- and 5.89-folds in slightly and severely infected stages respectively, compared to the healthy group (Fig. 2). This protein also contained a signal peptide at the N-terminus and is predicted as a secreted protein. The interaction between *Pyr. yezoensis* metalloproteinase inhibitor and *Pyt. porphyrae* metalloproteinase was simulated on database of three-dimensional interacting domains (3did, https://3did.irbbarcelona.org) using their protein sequences[39]. As shown in Fig. 3, TIMP (Tissue inhibitor of metalloproteinase, PF00965), the core domain of py03343.t1, could interact with the catalytic center (Peptidase_M10, PF00413) of metalloproteinase. This indicates that *Pyr. yezoensis* secretes py03343.t1 as extracellular metalloproteinase inhibitor to restrict the damage from pathogen metalloproteinase.

Secondary metabolism

F520, a marker for estimating plant secondary metabolite concentration in MCFI was measured during infection. Compared to the control group, F520 intensity of the infected group increased with a significant difference from 4 days post-infection when the lesion rate was only 3.7% and increased continuously with the spread of lesion (Fig. 4A). As shown in Fig. 4B, fluorescence images of F520 provide a visual representation of the secondary metabolite distribution in different infected stages. F520 increased

progressively from boundary to the center of the lesion. This indicates that *Pyr. yezoensis* could synthesize and accumulate secondary metabolites in response to infection.

The results were further confirmed by transcriptome data. Transcriptome analysis showed that eight genes related to phenolic biosynthesis were up-regulated significantly during infection (FC>1.5) (Fig. 2). The expression pattern of these genes was different between the slightly and severely infected stages. Three genes that were up-regulated only in the slightly infected stage, include luteolin and quercetin synthesis gene py07137.t1, isoquercetin synthesis gene py00829.t1, and 2-coumaric acid (precursor of coumarin) synthesis gene py05984.t1. Two genes that were up-regulated only in the severely infected stage are caffeoyl-CoA O-methyltransferase py04307.t1 and neohesperidin synthesis gene py00132.t1. However, another neohesperidin synthesis gene py01289.t1 was up-regulated both in the slightly and severely infected stage.

Heat shock proteins

The transcriptome data also showed that twelve heat shock protein genes (one HSP10, six HSP20s, one HSP40, two HSP70s, and two HSP90s) were up-regulated (FC>1.5) after infection (Fig. 2). Compared to the healthy control group, the expression of these HSP genes was increased significantly in both slightly and severely infected stages. Among them, HSP20s were the most highly up-regulated heat shock protein group in response to infection. Five out of six Hsp20 genes were up-regulated to more than 15-fold, specifically py04518.t1 and py08669.t1 up-regulated to ~200-fold post-infection.

Putative R proteins

Twenty-three *Pyr. yezoensis* transcripts containing typical R-protein domains such as LRR, NBS and TIR are summarized in Table 1. Among these genes, only one gene with LRR was up-regulated (FC=1.89) in slightly infected stage, three genes with NB-ARC+WD40 domain/motifs and one gene containing the TIR+Pkinase domain were up-regulated by more than 1.5-fold in both slightly and severely infected stages and one gene with NB-ARC+TPR was up-regulated only in severely infected stage (FC=2.31).

ETI mechanism in *Pyr. yezoensis*

In plants, hypersensitivity reaction (HR), a form of programmed cell death, is the key disease-resistance mechanism in ETI[40]. Metacaspases, a family of cysteine proteases, are described as the most important regulators of PCD in plants[41]. As shown in Fig. 5, the expression of two genes coding for metacaspase were significantly enhanced in slightly (FC=2.14) and severely infected stages (FC=1.84). Cytochrome C, considered the signal of mitochondrial apoptosis, was up-regulated (FC=2.7) in the severely infected stage. Furthermore, the gene encoding for mitochondrial endonuclease G was induced by 2.04- and 2.84-fold in slightly and severely infected stages, respectively.

Ubiquitination plays an essential role in plant PCD regulation. In *Pyr. yezoensis*, all processes related to ubiquitination system were up-regulated post- *Pyt. porphyrae* infection (Fig. 5). In the slightly infected stage, two ubiquitin genes, ubiquitin-conjugating enzyme UBE2A, UBE2C, and ubiquitin ligase UBE3C

displayed a significant up-regulation. In the severely infected stage, nine genes, that include five ubiquitin genes, ubiquitin-like activating enzyme UBLE1A, ubiquitin-conjugating enzyme UBE2A, UBE2C, and ubiquitin ligase UBE3C were all up-regulated by more than 1.5-fold.

Discussion

Conserved innate immune system in *Pyr. yezoensis*

Sensitive PTI mechanism

PTI, triggered by pathogenic PAMPs, are the first line of non-specific defense mechanism exhibited by the plant against the pathogen. In *Pyr. yezoensis*, after recognition of the carbohydrate PAMPs and lectin RLPs, PTI mechanism is activated in response to *Pyt. porphyrae* infection. Based on enrichment analysis, several broad-spectrum defense mechanisms could be identified in *Pyr. yezoensis*, including secondary metabolites, cellulase, metalloproteinase inhibitor, ROS, and HSPs. All these mechanisms were up regulated since the host was exposed to the zoospores at the slightly infected stage. This indicates that the *Pyr. yezoensis* PTI mechanism is extremely sensitive to infection.

Successful recognition of PAMPs and PRRs was the first step in the activation of innate immunity during infection in the plants [10]. Plant lectins play a crucial role in the recognition and binding of carbohydrate PAMPs. Based on the variability in lectin domains, lectin PRRs could be divided into three subclasses: L-type, G-type, and C-type. L-type lectins bind glucose/mannose (Glc/Man) specifically but the ligand PAMPs of G-type and C-type lectins are still not very evident in the plants[42]. During the infection, *Pyr. yezoensis* C-type lectin gene was up-regulated only in the slightly infected stage and L-type lectin genes were up-regulated only in the severely infected stage. Thus, suggesting that C-type lectin might recognize PAMPs expressed by *Pyt. porphyrae* and then modulate defense gene expression before direct invasion of the pathogen. L-type lectin might activate or amplify the PTI in severely infected stage by recognizing glucose and mannose released due to the degradation of the *Pyr. yezoensis* cell wall that consists of the mannan outer layer and xylan microfibrils in the inner layer [43, 44].

It has been reported that several secondary metabolites in red algae *Laurencia majuscule* exhibit antimicrobial activity against “ice-ice” bacteria [45]. In crops, secondary metabolites were frequently used to nondestructively detect diseases using MCFI [46, 47]. In the present study, MCFI was first used to measure the concentration of secondary metabolites in diseased algae. The results of F520 indicates *Pyr. yezoensis* induces secondary metabolite expression before direct invasion of the hyphae, suggesting that *Pyr. yezoensis* secondary metabolism is sensitive to *Pyt. porphyrae* infection and might be used in the nondestructive detection of red rot disease.

Protease inhibitors (PIs), a part of plant ETI, protect the host by inhibiting pathogen proteases and regulating the activity of host protease[48]. It has been proved that PIs from *Hordeum vulgare*, *Vicia faba,* and *A. thaliana* could inhibit the mycelial growth of several fungal pathogens (broad-spectrum inhibition) [49-51]. In the present study, an extracellular metalloproteinase inhibitor is identified for the first time in

the algal innate immune system. Consistent with the transcriptomic and proteomic data this protein expression was up-regulated significantly (FC=1.52) after infection (further analysis of data in [38]). It appears that *Pyr. yezoensis* secretes metalloproteinase inhibitor as a “bait” to occupy the metalloproteinase catalytic center and protects the host protein degradation by pathogen metalloproteinase.

Plants can inhibit the fungal pathogens by secreting chitinase and β-1, 3-glucanase that degrade fungal cell wall during infection[52, 53]. In *Pyr. tenera*, several cell-wall associated hydrolases were up-regulated after *Pyt. Porphyrae* invasion[37]. In the current study, we analyzed the pathogen cell wall degrading enzymes in detail. The main constituent of the oomycete cell wall is β-1,3-, β-1,4-, and β-1,6-linked glucan skeleton with cellulose and is different from the fungal cell wall. The *Pyr. yezoensis* cellulase belongs to glycosyl hydrolase family 5 (cellulase) and was continuously up-regulated during the whole infection process. It might be possible that *Pyr. yezoensis* secreted cellulase to degrade cellulose, thereby inhibiting the formation and expansion of *Pyt. porphyrae* hyphae.

Large HSPs and single R-protein domain-containing proteins act as R-proteins in Pyr. yezoensis

R proteins are essential for the plant to activate ETI and create specificity in disease resistance. R proteins with conserved protein structure are extensively present in higher plants. The increase in R-protein expression indicates the plausibility of these genes to be involved in *Pyr. yezoensis* innate immunity. However, owing to their simple protein structures, the function of these genes might be limited in the interaction of *Pyr. yezoensis* and *Pyt. porphyrae*.

Several findings demonstrated that large HSPs, such as HSP70s and HSP90s, could recognize pathogen effectors specifically and activate the defense mechanisms against pathogens [54]. Results from yeast two-hybrid analysis and co-immunoprecipitation indicate that HSP90s might play a role similar to R proteins in plants [55, 56]. Considering the absence of NBS-LRR proteins, the up-regulated HSP70s and HSP90s might serve as substitutes for a typical R protein in ETI activation of *Pyr. yezoensis* innate immune system.

Conversed ETI in Pyr. yezoensis

Hypersensitive response (HR), a form of programmed cell death, gets triggered after recognition of R protein and the effectors at the site of infection to prevent the spread of the pathogen[57]. It has been established that metacaspases are the key factors in plant PCD during infection. AtMC1 and AtMC2, two metacaspases in Arabidopsis, possess opposing roles in PCD during *Pseudomonas syringae* infection[58]. However, little is known about the mechanism of PCD in algae during biotic stress. Wang et al., hypothesized that flg22, a typical bacterial PAMP, could induce PCD in female gametophyte of *S. japonica* depending on the cell ultrastructural changes during infection[30]. It is well known that as an ETI mechanism, PCD is more efficient in resisting biotrophic pathogens but is limited in the defense against necrotrophic pathogens. As necrotrophic pathogens, *Pyt. porphyrae* could feed on the dead cells or tissues. Nevertheless, PCD related genes that were up-regulated include metacaspase, endonuclease G,

and cytochrome C, and these still could be identified in *Pyr. yezoensis* transcripts during infection. These results indicate that PCD is involved in the immune response of *Pyr. yezoensis* against *Pyt. porphyrae*.

In plants, UPS is associated with innate immunity mechanism in a variety of ways, such as PTI modulation, programmed cell death, and signal transduction[59]. E3 is the key enzyme in the process of ubiquitination as it binds to the target protein specifically via its target recognition subunit[60, 61]. In *Pyr. yezoensis*, genes related to UPS were up-regulated during infection. Especially in severely infected stage, all parts of UPS were up-regulated significantly, indicating that UPS might play a crucial role in *Pyr. yezoensis* to defend the invasion of *Pyt. porphyrae* hyphae in the severely infected stage.

The present study reasonably deduced the overall view of *Pyr. yezoensis* innate immunity (Fig. 6). During the slightly infected stage, *Pyr. yezoensis* cellulase is induced and secreted to degrade *Pyt. porphyrae* cell wall. Meanwhile, several types of oligosaccharides are produced that might be recognized as carbohydrate PAMPs by C-type lectins on the host membrane, these work in concert with an unknown kinase to activate the PTI mechanism. NADPH oxidase is induced to generate ROS. Meanwhile, antioxidase also is up-regulated to overcome oxidative stress. Secondary metabolism, especially the synthesis of phenolics is induced. A metalloproteinase inhibitor was shown to be highly induced and secreted to inhibit pathogen metalloproteinase activity. Several HSP20s, which are involved in damage repair, also are highly up-regulated. In severely infected stage, hyphae invade into cells of *Pyr. yezoensis*. Mannose gets released during the cell wall degradation of *Pyr. yezoensis*. Host L-type lectin recognizes the mannose to further activate and amplify the PTI mechanism. Besides, *Pyr. yezoensis* may rely on ETI to prevent the invasion of a pathogen. In *Pyr. yezoensis*, ETI gets activated by potential R-proteins containing typical R-protein domain. Hsp70s and HSP90s might play the role of R-proteins to interact with pathogen effectors. Similar to that seen in higher plants, in *Pyr. yezoensis* ETI, mechanisms described in the PTI were amplified. The ubiquitin system and PCD also get up-regulated to resist the infection.

The ancient origin of genes in the innate immune system of *Pyr. yezoensis*

Endosymbiosis drives the evolution and diversification of eukaryotic algae. Plastids originated from cyanobacteria and created three “primary algae”: Glaucophyta, Rhodophyta, and Chlorophyta. Chlorophyta further evolved to land plants[62]. The current study revealed that the defense mechanism in *Pyr. yezoensis* is similar to that seen in plants. Nevertheless, phylogenetic analysis revealed that the defense genes in *Pyr. yezoensis* might have an ancient origin.

PRRs are transmembrane proteins with functional ectodomains binding to PAMPs [63]. Based on whether the kinase domain is intracellular in origin or not, PRRs are classified into receptor-like kinases (RLKs) and receptor-like proteins (RLPs) in plants[64]. So far, all the identified lectin PRRs in plants belong to RLKs. However, due to the absence of intracellular kinase domain, lectins in *Pyr. yezoensis* belongs to RLPs. Phylogenetic analysis revealed that the *Pyr. yezoensis* lectin preserved ancient protein structure and originated earlier than plant lectins (Fig S2-S3). It has been reported that plant RLPs need an independent kinase to work together [64]. For instance, in tomato, Avr9/Cf-9 induced kinase 1 (ACIK1) is required to

interact with LRR-RLP *Cf-9* through the assistance of *Cf-9* interacting thioredoxin (CITRX) as a chaperone[65]. Therefore, we surmised that an unknown kinase is required to work with *Pyr. yezoensis* lectin to activate the downstream defense genes.

Nearly all the identified R proteins typically share commonly conversed domains of TNL (TIR-NBS- LRR) or nTNL (NBS- LRR)[17]. Recent studies analyzed the R protein in plants, Charophytes, Chlorophyta, Rhodophyta, and Glaucophyta[66, 67]. Proteins containing NBS or LRR domain are found to exist in all species. However, the fusion events of NBS and LRR domain was found in Chlorophyta and plants. This indicated that the origin of R protein could be traced back to Chlorophyta, such as *Chromochloris zofingiensis* and *Botryococcus braunii* [67]. In the current study, six up-regulated genes encoding NBS, LRR, or TIR containing proteins were predicted as R protein candidates in *Pyr. yezoensis*. As shown in Figure S4, these genes originate anciently compared to typical R proteins in plants. Structural analysis showed that all these genes encode an ancient protein structure of a single R protein domain without fusion events. The phenomenon of gene fusion was generally found during the evolution of organisms. In archaea and bacteria, the glutamyl- and prolyl-tRNA synthetases (GluRS and ProRS) are encoded by two distinct genes. However, a single polypeptide chain protein combining GluRS and ProRS were present in the eukaryotic phylum of coelomate metazoans[68]. Similar co-working mechanism also exists in *Arabidopsis* R proteins. Due to the lack of LRR, TIR-NBS and TIR-X proteins could interact with NBS-LRR[69]. This suggests that proteins containing a single R protein domain could also act as R proteins with the assistance of other proteins. Therefore, we assumed that single domain containing protein (NBS, TIR, or LRR) might play the role of R protein by working in concert.

As shown in Figure S5–S7, the PTI genes of *Pyr. yezoensis*, that include cellulase, metalloproteinase inhibitor, and NADH-oxidase were clustered into a clade of Rhodophyta, which is separate from the clade of plants and Chlorophyta. Therefore, our findings indicate that *Pyr. yezoensis* defense genes preserve the original character in the evolutionary process of plant innate immune system.

Conclusions

In the current study, we outlined the innate immune system of red alga *Pyr. yezoensis* based on the transcriptomic data during the red rot disease. The conserved defense mechanisms seen in higher plants were also revealed in the red algae. *Pyr. yezoensis* lectins might act as PRRs to activate PTI after the recognition of carbohydrate PAMPs. PTI mechanisms include the up-regulation of ROS, secondary metabolism, metalloproteinase inhibitor, cellulase and small HSPs in response to infection. PCD and UPS, as ETI, might be activated as a defense mechanism to infection after effector recognition by putative R proteins and HSP70s. Nevertheless, compared to the homologs in higher plants, *Pyr. yezoensis* defense genes appeared to have ancient characteristics. The protein structure of pathogen receptors, that include PRRs and R proteins, were simple with a single functional domain. Therefore, our study provides valuable clues not only for understanding the innate immunity mechanisms of red algae, but also for tracing back the origin of the innate immune system in plants.

Abbreviations

PRRs: pattern recognition receptors

PAMPs: pathogen-associated molecular patterns

PTI: PAMP-triggered immunity

ETS: effector-triggered susceptibility

ETI: Effector-triggered immunity

LRR: leucine rich repeat

NBS: nucleotide binding site

TIR: Toll/interleukin-1 receptor like

UPS: ubiquitin-proteasome system

HR: hypersensitive response

ROS: reactive oxygen species

POD: Peroxidase

CAT: Catalase

SOD: Superoxide Dismutase

HSP: Heat shock protein

FC: Fold change

MCFI: Multi-color fluorescence imaging

References

1. Chen, Q., W. Guo, L. Feng, X. Ye, W. Xie, X. Huang, and J. Liu, Transcriptome and proteome analysis of Eucalyptus infected with *Calonectria pseudoreteaudii*. Journal of proteomics, 2015. 115: p. 117-131.
2. Ma, X., B. Keller, B.A. McDonald, J. Palma-Guerrero, and T. Wicker, Comparative transcriptomics reveals how wheat responds to infection by *Zymoseptoria tritici*. Molecular plant-microbe interactions, 2018. 31(4): p. 420-431.
3. Zhu, Q., P. Gao, Y. Wan, H. Cui, C. Fan, S. Liu, and F. Luan, Comparative transcriptome profiling of genes and pathways related to resistance against powdery mildew in two contrasting melon

genotypes. Scientia horticulturae, 2018. 227: p. 169-180.

4. Cook, R., J. Sitton, and J. Waldher, Evidence for Pythium as a pathogen of direct-drilled wheat in the Pacific Northwest. Plant Dis, 1980. 64(1): p. 61-61.
5. Zuluaga, A.P., J.C. Vega-Arreguín, Z. Fei, A.J. Matas, S. Patev, W.E. Fry, and J.K. Rose, Analysis of the tomato leaf transcriptome during successive hemibiotrophic stages of a compatible interaction with the oomycete pathogen *Phytophthora infestans*. Molecular plant pathology, 2016. 17(1): p. 42-54.
6. Duan, K., C.J. Willig, J.R. De Tar, W.G. Spollen, and Z.J. Zhang, Transcriptomic analysis of Arabidopsis seedlings in response to an Agrobacterium-mediated transformation process. Molecular plant-microbe interactions, 2018. 31(4): p. 445-459.
7. Li, X., M. An, Z. Xia, X. Bai, and Y. Wu, Transcriptome analysis of watermelon (*Citrullus lanatus*) fruits in response to Cucumber green mottle mosaic virus (CGMMV) infection. Scientific reports, 2017. 7(1): p. 16747.
8. Li, Y., X. Hu, J. Chen, W. Wang, X. Xiong, and C. He, Integrated mRNA and microRNA transcriptome analysis reveals miRNA regulation in response to PVA in potato. Scientific reports, 2017. 7(1): p. 16925.
9. Takebe, I. and Y. Otsuki, Infection of tobacco mesophyll protoplasts by tobacco mosaic virus. Proceedings of the National Academy of Sciences, 1969. 64(3): p. 843-848.
10. Jones, J.D. and J.L. Dangl, The plant immune system. nature, 2006. 444(7117): p. 323.
11. Beckman, C., W. Mueller, B. Tessier, and N. Harrison, Recognition and callose deposition in response to vascular infection in fusarium wilt-resistant or susceptible tomato plants. Physiological Plant Pathology, 1982. 20(1): p. 1-10.
12. Ellinger, D., M. Naumann, C. Falter, C. Zwikowics, T. Jamrow, C. Manisseri, S.C. Somerville, and C.A. Voigt, Elevated early callose deposition results in complete penetration resistance to powdery mildew in Arabidopsis. Plant physiology, 2013. 161(3): p. 1433-1444.
13. Samalova, M., H. Mélida, F. Vilaplana, V. Bulone, D.M. Soanes, N.J. Talbot, and S.J. Gurr, The β-1, 3-glucanosyltransferases (Gels) affect the structure of the rice blast fungal cell wall during appressorium-mediated plant infection. Cellular microbiology, 2017. 19(3): p. e12659.
14. Tu, J. and C. Hiruki, Electron microscopy of cell wall thickening in local lesions of potato virus-M infected red kidney bean. virus, 1971. 8: p. 20.
15. Lehmann, S., M. Serrano, F. L'Haridon, S.E. Tjamos, and J.-P. Metraux, Reactive oxygen species and plant resistance to fungal pathogens. Phytochemistry, 2015. 112: p. 54-62.
16. Li, Y.-B., L.-B. Han, H.-Y. Wang, J. Zhang, S.-T. Sun, D.-Q. Feng, C.-L. Yang, Y.-D. Sun, N.-Q. Zhong, and G.-X. Xia, The thioredoxin GbNRX1 plays a crucial role in homeostasis of apoplastic reactive oxygen species in response to *Verticillium dahliae* infection in cotton. Plant physiology, 2016. 170(4): p. 2392-2406.
17. Gururani, M.A., J. Venkatesh, C.P. Upadhyaya, A. Nookaraju, S.K. Pandey, and S.W. Park, Plant disease resistance genes: current status and future directions. Physiological and molecular plant pathology, 2012. 78: p. 51-65.

18. Ding, H. and J. Ma, Simultaneous infection by red rot and chytrid diseases in *Porphyra yezoensis* Ueda. Journal of Applied Phycology, 2005. 17(1): p. 51-56.
19. Suttle, C.A., A.M. Chan, and M.T. Cottrell, Infection of phytoplankton by viruses and reduction of primary productivity. Nature, 1990. 347(6292): p. 467.
20. Wang, G., L. Shuai, Y. Li, W. Lin, X. Zhao, and D. Duan, Phylogenetic analysis of epiphytic marine bacteria on Hole-Rotten diseased sporophytes of *Laminaria japonica*. Journal of applied phycology, 2008. 20(4): p. 403-409.
21. Grenville-Briggs, L., C.M. Gachon, M. Strittmatter, L. Sterck, F.C. Küpper, and P. van West, A molecular insight into algal-oomycete warfare: cDNA analysis of *Ectocarpus siliculosus* infected with the basal oomycete *Eurychasma dicksonii.* PLoS One, 2011. 6(9): p. e24500.
22. Strittmatter, M., L.J. Grenville-Briggs, L. Breithut, P. Van West, C.M. Gachon, and F.C. Küpper, Infection of the brown alga *Ectocarpus siliculosus* by the oomycete *Eurychasma dicksonii* induces oxidative stress and halogen metabolism. Plant, cell & environment, 2016. 39(2): p. 259-271.
23. Tsirigoti, A., G.W. Beakes, C. Hervé, C.M. Gachon, and C. Katsaros, Attachment, penetration and early host defense mechanisms during the infection of filamentous brown algae by *Eurychasma dicksonii*. Protoplasma, 2015. 252(3): p. 845-856.
24. Tsirigoti, A., F. Küpper, C. Gachon, and C. Katsaros, Cytoskeleton organisation during the infection of three brown algal species, *Ectocarpus siliculosus*, *Ectocarpus crouaniorum* and *Pylaiella littoralis*, by the intracellular marine oomycete *Eurychasma dicksonii*. Plant Biology, 2014. 16(1): p. 272-281.
25. Küpper, F.C., B. Kloareg, J. Guern, and P. Potin, Oligoguluronates elicit an oxidative burst in the brown algal kelp *Laminaria digitata*. Plant physiology, 2001. 125(1): p. 278-291.
26. Küpper, F.C., D.G. Müller, A.F. Peters, B. Kloareg, and P. Potin, Oligoalginate recognition and oxidative burst play a key role in natural and induced resistance of sporophytes of Laminariales. Journal of chemical ecology, 2002. 28(10): p. 2057-2081.
27. Goulitquer, S., A. Ritter, F. Thomas, C. Ferec, J.P. Salaün, and P. Potin, Release of volatile aldehydes by the brown algal kelp *Laminaria digitata* in response to both biotic and abiotic stress. ChemBioChem, 2009. 10(6): p. 977-982.
28. Cosse, A., P. Potin, and C. Leblanc, Patterns of gene expression induced by oligoguluronates reveal conserved and environment-specific molecular defense responses in the brown alga *Laminaria digitata*. New Phytologist, 2009. 182(1): p. 239-250.
29. Liu, C., L. Wang, M. Wang, and X. Tang, Difference analysis of infection activity of alginic acid decomposing bacteria infecting *Laminaria japonica*. Marine Sciences, 2002. 26(6): p. 44-47.
30. Wang, S., F. Zhao, X. Wei, B. Lu, D. Duan, and G. Wang, Preliminary study on flg22-induced defense responses in female gametophytes of *Saccharina japonica* (Phaeophyta). Journal of applied phycology, 2013. 25(4): p. 1215-1223.
31. Mo, Z., S. Li, F. Kong, X. Tang, and Y. Mao, Characterization of a novel fungal disease that infects the gametophyte of *Pyropia yezoensis* (Bangiales, Rhodophyta). Journal of applied phycology, 2016. 28(1): p. 395-404.

32. Klochkova, T.A., Y.J. Shin, K.-H. Moon, T. Motomura, and G.H. Kim, New species of unicellular obligate parasite, *Olpidiopsis pyropiae* sp. nov., that plagues Pyropia sea farms in Korea. Journal of applied phycology, 2016. 28(1): p. 73-83.
33. Guan, X., J. Li, Z. Zhang, F. Li, R. Yang, P. Jiang, and S. Qin, Characterizing the microbial culprit of white spot disease of the conchocelis stage of *Porphyra yezoensis* (Bangiales, Rhodophyta). Journal of applied phycology, 2013. 25(5): p. 1341-1348.
34. Arasaki, S., Studies on the rot of *Porohyra tenera* by Pythium. Nippon Suisan Gakkaishi, 1947. 13: p. 74-90.
35. Qiu, L., Y. Mao, L. Tang, X. Tang, and Z. Mo, Characterization of *Pythium chondricola* associated with red rot disease of *Pyropia yezoensis* (Ueda)(Bangiales, Rhodophyta) from Lianyungang, China. Journal of Oceanology and Limnology, 2019. 37(3): p. 1102-1112.
36. Park, C.S. and E.K. Hwang, Isolation and evaluation of a strain of *Pyropia yezoensis* (Bangiales, Rhodophyta) resistant to red rot disease. Journal of applied phycology, 2014. 26(2): p. 811-817.
37. Im, S.H., T.A. Klochkova, D.J. Lee, C.M. Gachon, and G.H. Kim, Genetic toolkits of the red alga *Pyropia tenera* against the three most common diseases in Pyropia farms. Journal of phycology, 2019.
38. Khan, S., Y. Mao, D. Gao, S. Riaz, Z. Niaz, L. Tang, S. Khan, and D. Wang, Identification of proteins responding to pathogen-infection in the red alga *Pyropia yezoensis* using iTRAQ quantitative proteomics. BMC genomics, 2018. 19(1): p. 842.
39. Mosca, R., A. Ceol, A. Stein, R. Olivella, and P. Aloy, 3did: a catalog of domain-based interactions of known three-dimensional structure. Nucleic acids research, 2013. 42(D1): p. D374-D379.
40. Coll, N., P. Epple, and J. Dangl, Programmed cell death in the plant immune system. Cell death and differentiation, 2011. 18(8): p. 1247.
41. Fagundes, D., B. Bohn, C. Cabreira, F. Leipelt, N. Dias, M.H. Bodanese-Zanettini, and A. Cagliari, Caspases in plants: metacaspase gene family in plant stress responses. Functional & integrative genomics, 2015. 15(6): p. 639-649.
42. Vaid, N., A. Macovei, and N. Tuteja, Knights in action: lectin receptor-like kinases in plant development and stress responses. Molecular plant, 2013. 6(5): p. 1405-1418.
43. Frei, E. and R.D. Preston, Non-cellulosic structural polysaccharides in algal cell walls-II. Association of xylan and mannan in *Porphyra umbilicalis*. Proceedings of the Royal Society of London. Series B. Biological Sciences, 1964. 160(980): p. 314-327.
44. Mukai, L.S., J.S. Craigie, and R.G. Brown, Chemical composition and structure of the cell walls of the conchocelis and thallus phases of *Porohyra tenera* (Rhodophyceae) 1, 2. Journal of Phycology, 1981. 17(2): p. 192-198.
45. Vairappan, C.S., S.P. Anangdan, K.L. Tan, and S. Matsunaga, Role of secondary metabolites as defense chemicals against ice-ice disease bacteria in biofouler at carrageenophyte farms. Journal of applied phycology, 2010. 22(3): p. 305-311.
46. Pérez-Bueno, M.L., M. Pineda, F.M. Cabeza, and M. Barón, Multicolor fluorescence imaging as a candidate for disease detection in plant phenotyping. Frontiers in plant science, 2016. 7: p. 1790.

47. Pineda, M., M.L. Pérez-Bueno, V. Paredes, and M. Barón, Use of multicolour fluorescence imaging for diagnosis of bacterial and fungal infection on zucchini by implementing machine learning. Functional plant biology, 2017. 44(6): p. 563-572.
48. Kim, J.-Y., S.-C. Park, I. Hwang, H. Cheong, J.-W. Nah, K.-S. Hahm, and Y. Park, Protease inhibitors from plants with antimicrobial activity. International journal of molecular sciences, 2009. 10(6): p. 2860-2872.
49. Laluk, K. and T. Mengiste, The Arabidopsis extracellular UNUSUAL SERINE PROTEASE INHIBITOR functions in resistance to necrotrophic fungi and insect herbivory. The Plant Journal, 2011. 68(3): p. 480-494.
50. Pekkarinen, A.I., C. Longstaff, and B.L. Jones, Kinetics of the inhibition of Fusarium serine proteinases by barley (*Hordeum vulgare* L.) inhibitors. Journal of agricultural and food chemistry, 2007. 55(7): p. 2736-2742.
51. Ye, X., T. Ng, and P. Rao, A Bowman–Birk-type trypsin-chymotrypsin inhibitor from broad beans. Biochemical and biophysical research communications, 2001. 289(1): p. 91-96.
52. Anand, A., T. Zhou, H.N. Trick, B.S. Gill, W.W. Bockus, and S. Muthukrishnan, Greenhouse and field testing of transgenic wheat plants stably expressing genes for thaumatin-like protein, chitinase and glucanase against F*usarium graminearum*. Journal of Experimental Botany, 2003. 54(384): p. 1101-1111.
53. Grison, R., B. Grezes-Besset, M. Schneider, N. Lucante, L. Olsen, J.-J. Leguay, and A. Toppan, Field tolerance to fungal pathogens of *Brassica napus* constitutively expressing a chimeric chitinase gene. Nature biotechnology, 1996. 14(5): p. 643.
54. Goldberg, A.L., Protein degradation and protection against misfolded or damaged proteins. Nature, 2003. 426(6968): p. 895.
55. Bieri, S., S. Mauch, Q.-H. Shen, J. Peart, A. Devoto, C. Casais, F. Ceron, S. Schulze, H.-H. Steinbiß, and K. Shirasu, RAR1 positively controls steady state levels of barley MLA resistance proteins and enables sufficient MLA6 accumulation for effective resistance. The Plant Cell, 2004. 16(12): p. 3480-3495.
56. De La Fuente Bentem van, S., J.H. Vossen, K.J. de Vries, S. van Wees, W.I. Tameling, H.L. Dekker, C.G. de Koster, M.A. Haring, F.L. Takken, and B.J. Cornelissen, Heat shock protein 90 and its co-chaperone protein phosphatase 5 interact with distinct regions of the tomato I-2 disease resistance protein. The Plant Journal, 2005. 43(2): p. 284-298.
57. Goodman, R.N. and A.J. Novacky, The hypersensitive reaction in plants to pathogens: a resistance phenomenon. 1994: American Phytopathological Society (APS).
58. Coll, N., A. Smidler, M. Puigvert, C. Popa, M. Valls, and J. Dangl, The plant metacaspase AtMC1 in pathogen-triggered programmed cell death and aging: functional linkage with autophagy. Cell death and differentiation, 2014. 21(9): p. 1399.
59. Vierstra, R.D., The ubiquitin–26S proteasome system at the nexus of plant biology. Nature Reviews Molecular Cell Biology, 2009. 10(6): p. 385.

60. Craig, A., R. Ewan, J. Mesmar, V. Gudipati, and A. Sadanandom, E3 ubiquitin ligases and plant innate immunity. Journal of experimental botany, 2009. 60(4): p. 1123-1132.
61. Mazzucotelli, E., S. Belloni, D. Marone, A. De Leonardis, D. Guerra, N. Di Fonzo, L. Cattivelli, and A. Mastrangelo, The E3 ubiquitin ligase gene family in plants: regulation by degradation. Current genomics, 2006. 7(8): p. 509-522.
62. Bhattacharya, D., H.S. Yoon, and J.D. Hackett, Photosynthetic eukaryotes unite: endosymbiosis connects the dots. Bioessays, 2004. 26(1): p. 50-60.
63. Jones, D.A. and D. Takemoto, Plant innate immunity–direct and indirect recognition of general and specific pathogen-associated molecules. Current opinion in immunology, 2004. 16(1): p. 48-62.
64. Zipfel, C., Pattern-recognition receptors in plant innate immunity. Current opinion in immunology, 2008. 20(1): p. 10-16.
65. Nekrasov, V., A.A. Ludwig, and J.D. Jones, CITRX thioredoxin is a putative adaptor protein connecting Cf-9 and the ACIK1 protein kinase during the Cf-9/Avr9-induced defence response. FEBS letters, 2006. 580(17): p. 4236-4241.
66. Gao, Y., W. Wang, T. Zhang, Z. Gong, H. Zhao, and G.-Z. Han, Out of water: The origin and early diversification of plant R-genes. Plant physiology, 2018. 177(1): p. 82-89.
67. Shao, Z.-Q., J.-Y. Xue, Q. Wang, B. Wang, and J.-Q. Chen, Revisiting the origin of plant NBS-LRR genes. Trends in plant science, 2019. 24(1): p. 9-12.
68. Berthonneau, E. and M. Mirande, A gene fusion event in the evolution of aminoacyl-tRNA synthetases. FEBS letters, 2000. 470(3): p. 300-304.
69. Nandety, R.S., J.L. Caplan, K. Cavanaugh, B. Perroud, T. Wroblewski, R.W. Michelmore, and B.C. Meyers, The role of TIR-NBS and TIR-X proteins in plant basal defense responses. Plant physiology, 2013. 162(3): p. 1459-1472.
70. Provasoli, L. Media and prospects for the cultivation of marine algae. in Cultures and Collections of Algae. Proceedings of US-Japan Conference, Hakone, September 1966. 1968. Japan Society of Plant Physiology.
71. Fujita, Y. and B. Zenitani, Studies on pathogenic Pythium of laver red rot in ariake sea farm. 2. Experimental conditions and nutritional-requirements for growth. Bulletin of the Japanese Society of Scientific Fisheries, 1977. 43(1): p. 89-95.
72. Addepalli, M. and Y. Fujita, Regulatory role of external calcium on *Pythium porphyrae* (Oomycota) zoospore release, development and infection in causing red rot disease of *Porphyra yezoensis* (Rhodophyta). FEMS microbiology letters, 2002. 211(2): p. 253-257.
73. Emanuelsson, O., S. Brunak, G. Von Heijne, and H. Nielsen, Locating proteins in the cell using TargetP, SignalP and related tools. Nature protocols, 2007. 2(4): p. 953.
74. Nielsen, H., Predicting secretory proteins with SignalP, in Protein function prediction. 2017, Springer. p. 59-73.

75. Petersen, T.N., S. Brunak, G. Von Heijne, and H. Nielsen, SignalP 4.0: discriminating signal peptides from transmembrane regions. Nature methods, 2011. 8(10): p. 785.
76. Uppalapati, S., J. Kerwin, and Y. Fujita, Epifluorescence and scanning electron microscopy of host-pathogen interactions between *Pythium porphyrae* (Peronosporales, Oomycota) and *Porphyra yezoensis* (Bangiales, Rhodophyta). Botanica Marina, 2001. 44(2): p. 139-145.

Declarations

Ethics approval and consent to participate

Not applicable

Consent for publication

Not applicable

Availability of data and materials

The datasets generated during the current study are available in the Sequence Read Archive (SRA) repository accessible through NCBI BioProject ID PRJNA560692 (https://dataview.ncbi.nlm.nih.gov/object/PRJNA560692?reviewer=99tc7nravboeun8gna76hrjorp).

Competing interests

The authors declare that they have no competing interests.

Funding

This work was financially supported by the National Key R&D Program of China (2018YFD0900106, 2018YFC1406700), the Marine S&T Fund of Shandong Province for Pilot National Laboratory for Marine Science and Technology (Qingdao) (No. 2018SDKJ0302-4), the Fundamental Research Funds for the Central Universities (201762016), the MOA Modern Agricultural Talents Support Project.

Authors' contributions

YM designed of the work, LT and QP performed the experiments, LT and CL analyzed the data, YM, ZL and LT drafted and revised the manuscript. All authors are in agreement with the final manuscript.

Acknowledgments

Not applicable

Tables

Table 1. Expression and annotation of putative R proteins in *Pyr. yezoensis*

Gene ID	Typical Domain	Fold change (Slightly infected/ Healthy)	Fold change (Severely infected/ Healthy)	Protein domains
py02473.t1	LRR	1.89*	0.79	LRR
py00537.t1		1.33	1.09	LRR
py04246.t1		1.32	1.1	LRR
py08953.t1		1.27	1.27	LRR
py09599.t1		1.09	0.74	LRR
py07189.t1		0.9	0.8	LRR+ Hyl III
py10098.t1		0.91	1.1	LRR
py04256.t1		0.85	0.7	LRR
py07266.t1		0.84	0.78	LRR
py09987.t1		0.83	1.13	LRR
py00198.t1		0.81	1.02	LRR
py02537.t1	NBS	2.17*	1.69*	NB-ARC+ WD40
py00496.t1		1.69*	1.74*	NB-ARC+WD40
py07098.t1		1.64*	1.52*	NB-ARC+WD40
py11015.t1		1.47	1.38	NB-ARC+TPR
py07097.t1		1.37	1.17	NB-ARC+WD40
py04459.t1		1.27	2.31*	NB-ARC+TPR
py10255.t1		1.25	1.3	NB-ARC+WD40
py11066.t1		1.21	0.75	NB-ARC+WD40
py07671.t1		1.11	1.06	Trypsin+ NB-ARC+TPR+ elF2
py00971.t1		1.06	1.24	NB-ARC+TPR
py04439.t1		1.05	1.42	NB-ARC+WD40
py01330.t1	TIR	1.51*	1.59*	TIR+Pkinase
py08661.t1		1	1.27	TIR+Pkinase

*: significant change of FMPK(≥1.5-fold or ≤0.67-fold)

Figures

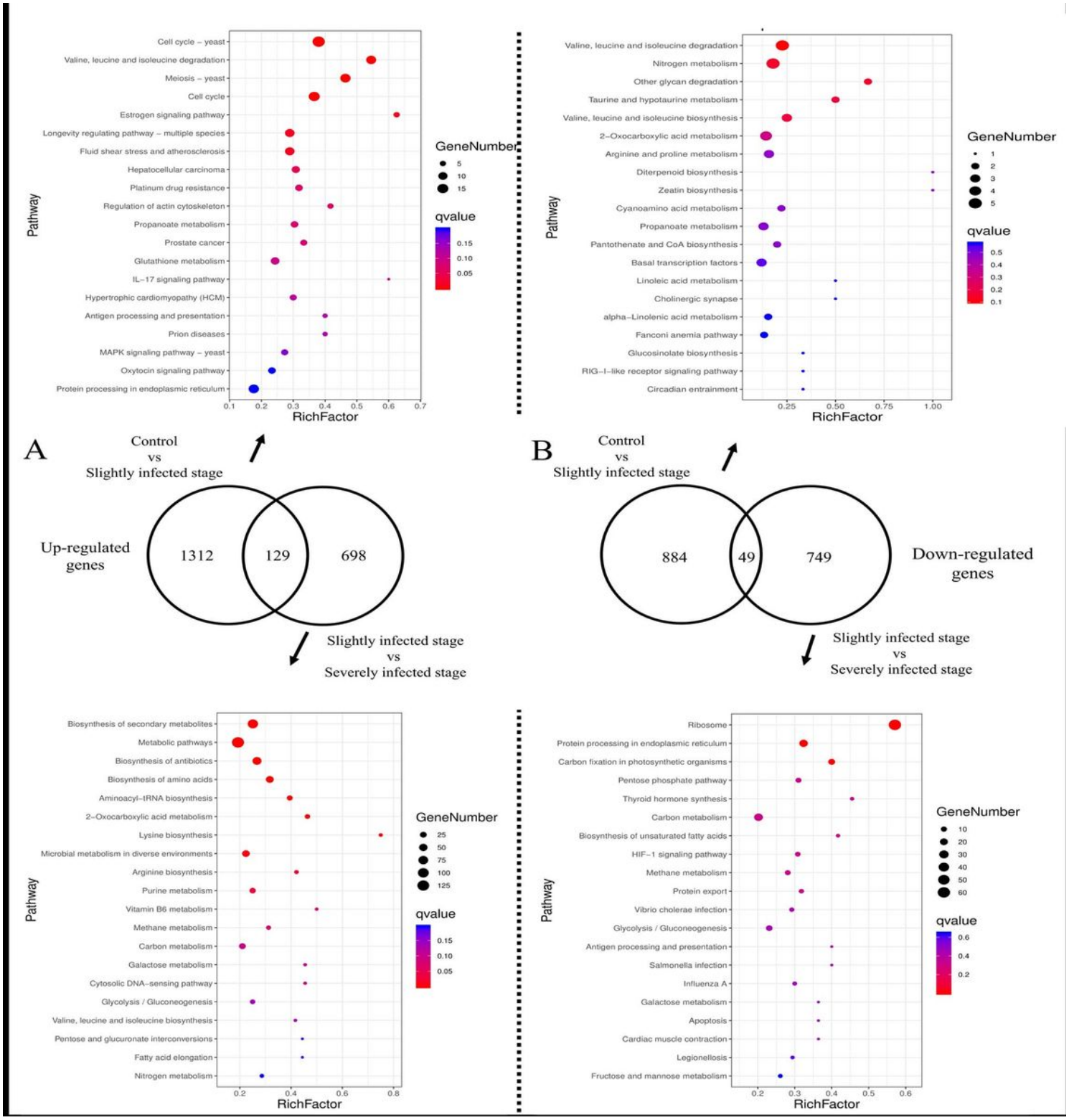

Figure 1

Venn diagram of differential expressed genes and the top 20 pathways of KEGG enrichment. A. Up-regulated genes; B. Down-regulated genes.

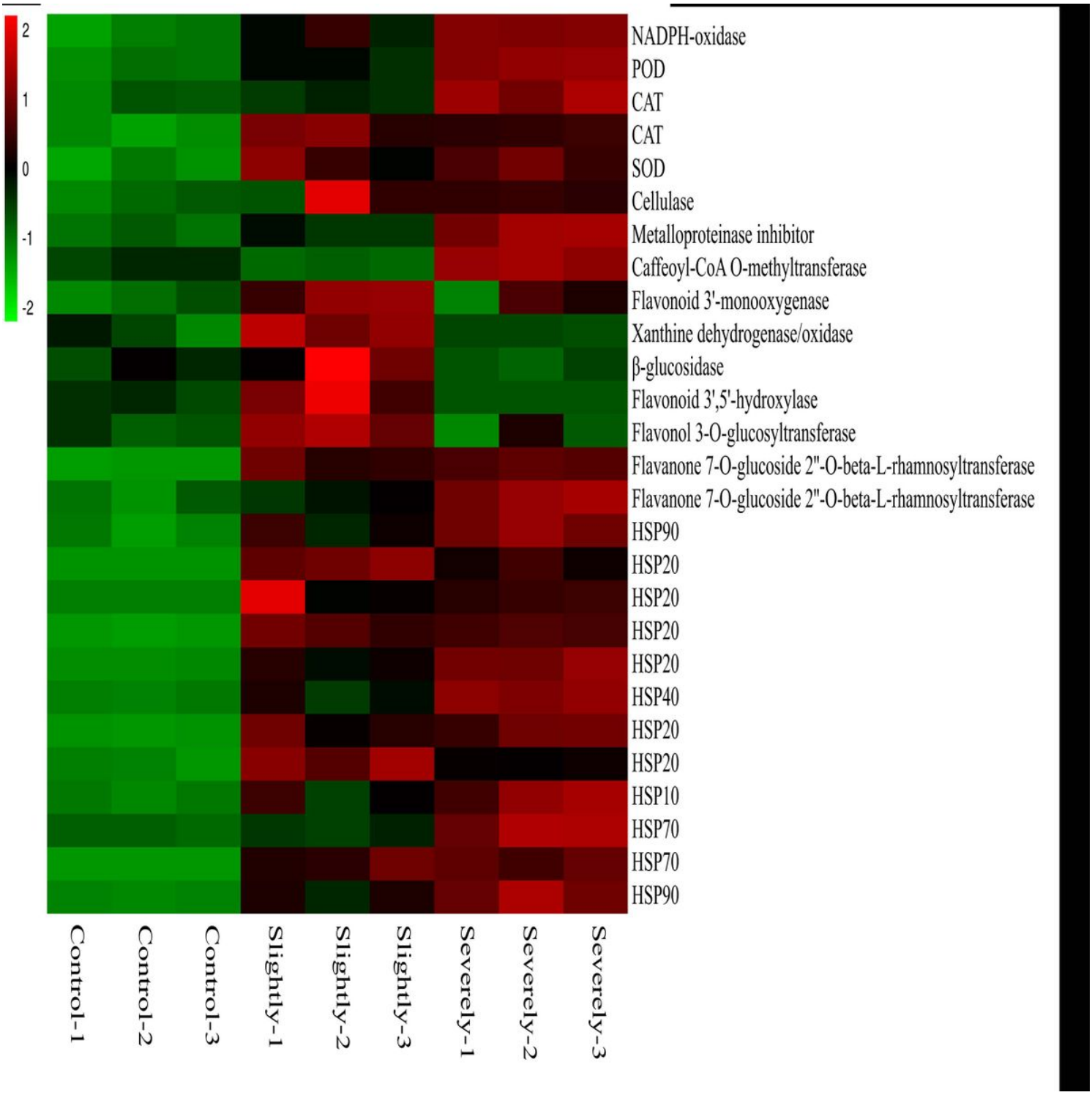

Figure 2

Heatmap of genes related to PTI in Pyr. yezoensis during infection. Differential expression is represented in different colors. A negative number indicates down-regulated genes and the positive number represents up-regulated genes. POD: Peroxidase; CAT: Catalase; SOD: Superoxide Dismutase; HSP: Heat shock protein

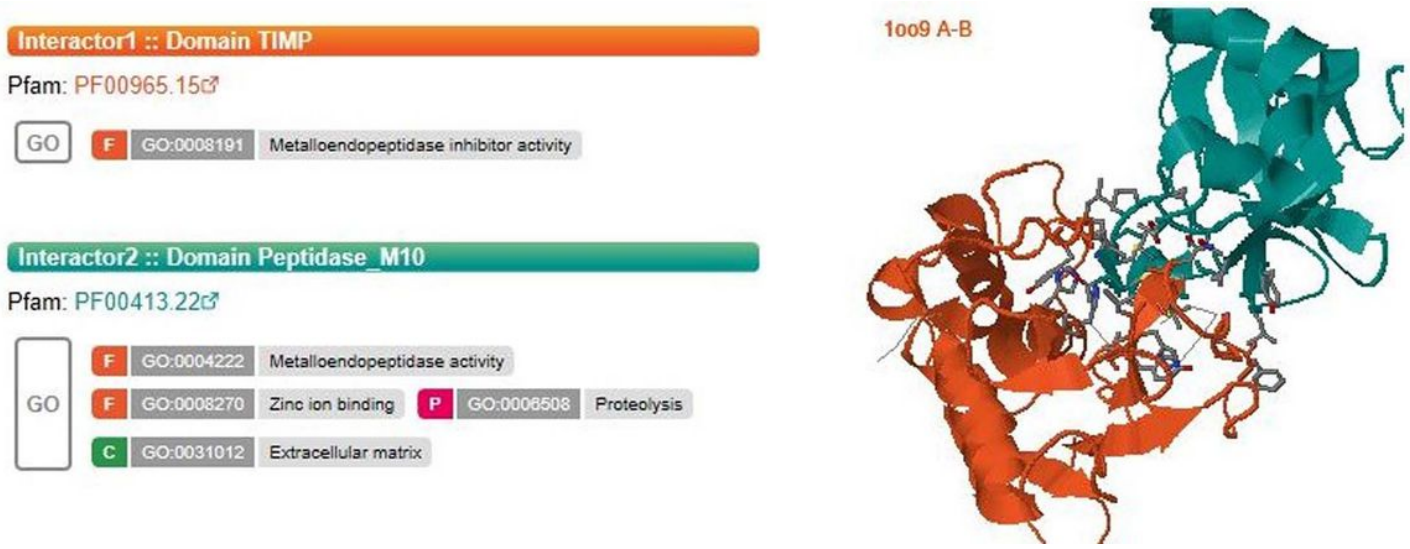

Figure 3

Interaction of Pyr. yezoensis metalloproteinase inhibitor and Pyt. porphyrae metalloproteinase. The interaction was simulated on database of 3did. Typical domains of the two proteins are shown as interactor1 and interactor2 in the left column. 3D image of interaction of the two proteins is shown in the right column.

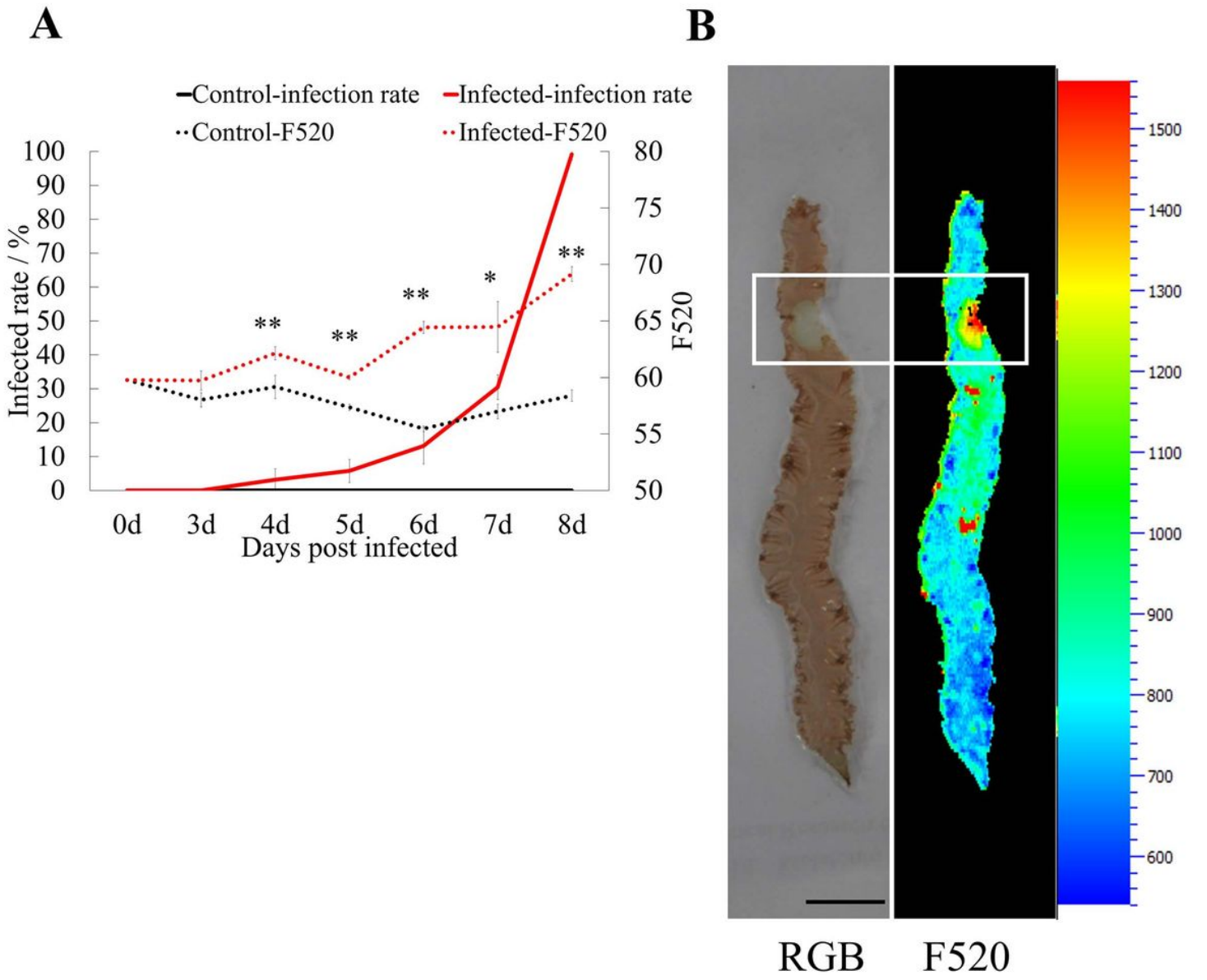

Figure 4

Up-regulated secondary metabolism in Pyr. yezoensis after infection A. F520 and infection rate during the infection process. * and ** stand for the significant difference of $p<0.05$ and 0.01, respectively. B. Secondary metabolism of infected Pyr. yezoensis by Multicolor Fluorescence Imaging. RGB: Red, green, blue (RGB) images showing the lesion; F520: Images of green fluorescence (F520). F520 images of the lesion are highlighted by a white rectangle.

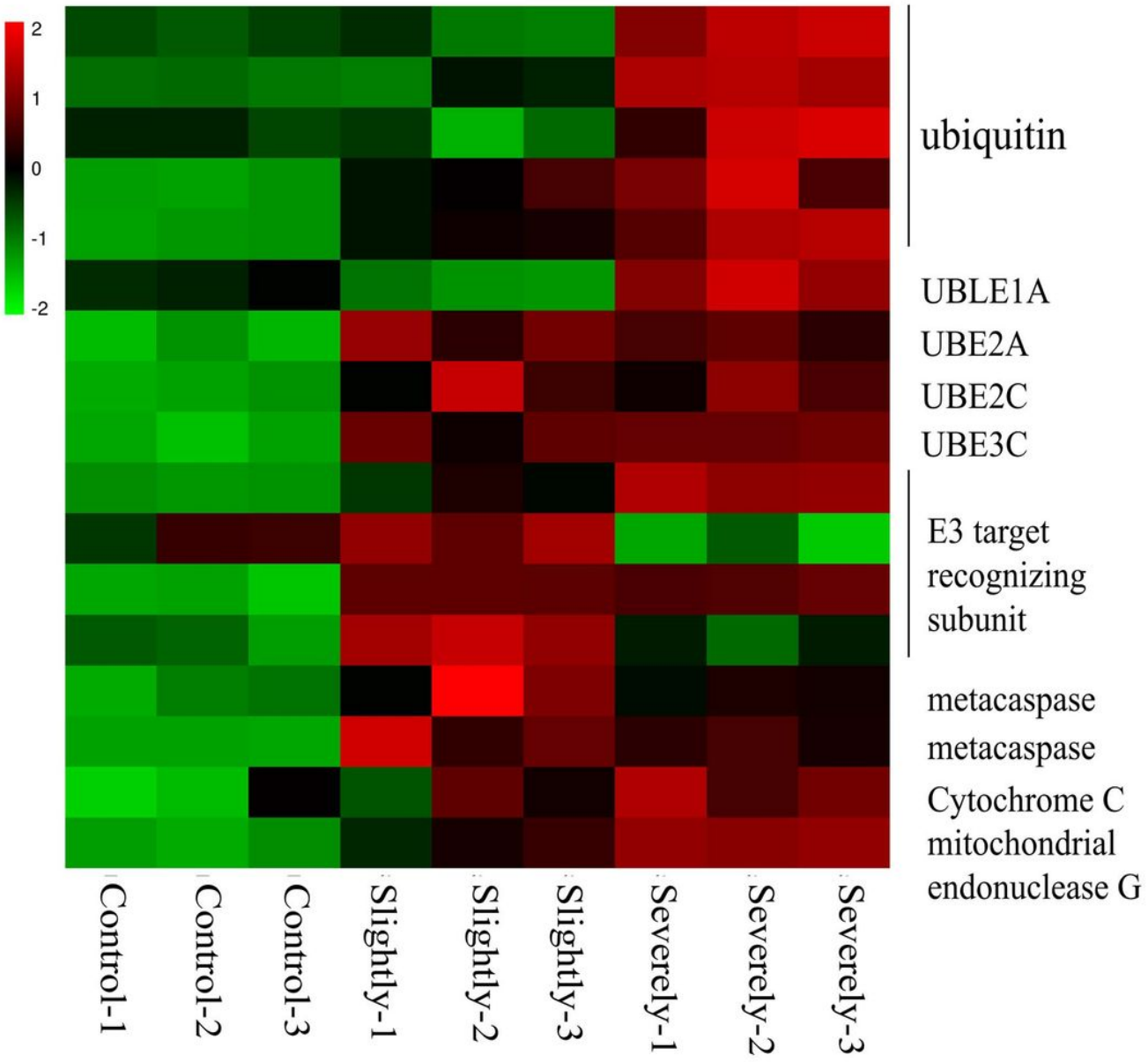

Figure 5

Heatmap of genes related to ubiquitination and programmed cell death in Pyr. yezoensis during infection. Differential expression is shown in different colors. A negative number indicates down-regulation of genes and the positive number indicates up-regulation of genes. Three biological replicates for control, slightly infected and severely infected stages are shown.

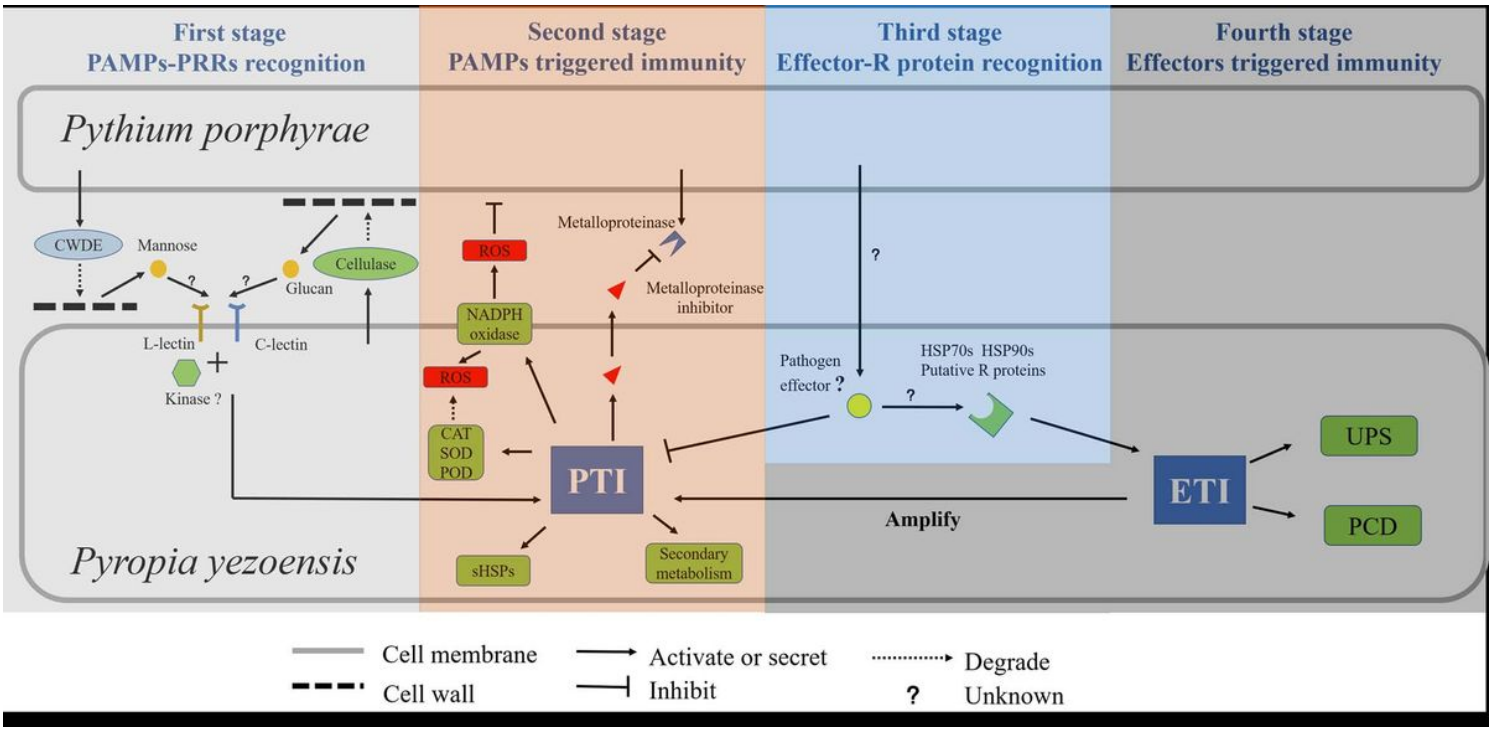

Figure 6

Overall view of Pyr. yezoensis innate immune system during Pyt. Porphyrae infection. The entire process of innate immunity in Pyr. yezoensis during infection of Pyt. porphyrae is depicted. First stage: carbohydrate PAMPs released during cell wall degradation is recognized by lectin RLPs. Second stage: with the co-work of kinase, PTI gets activated. Third stage: putative R proteins or large HSPs may recognize the pathogen effectors and activate the ETI. Fourth stage: genes related to UPS and HR are up-regulated. PTI is also amplified. PAMPs: pathogen-associated molecular patterns; CWDE: cell wall degrading enzymes; PTI: PAMPs triggered immunity; ROS: reactive oxygen species; CAT: catalase; SOD: superoxide dismutase; POD: peroxidase; sHSPs: small heat shock proteins; ETI: effectors triggered immunity; UPS: ubiquitin-proteasome system; PCD: programmed cell death.

Supplementary Files

This is a list of supplementary files associated with this preprint. Click to download.

- Additionalfiles8FIGS6.tif
- Additionalfiles2TableS1.docx
- Additionalfiles1.docx
- Additionalfiles4FIGS2.tif
- Additionalfiles3FIGS1.tif
- Additionalfiles5FIGS3.tif
- Additionalfiles7FIGS5.tif

- Additionalfiles6FIGS4.tif
- Additionalfiles9FIGS7.tif